Angewandte Chemie
Eine Zeitschrift der Gesellschaft Deutscher Chemiker

Supporting Information

Stiffness Tomography of Ultra-Soft Nanogels by Atomic Force Microscopy

*M. Friederike Schulte, Steffen Bochenek, Monia Brugnoni, Andrea Scotti, Ahmed Mourran, and Walter Richtering**

anie_202011615_sm_miscellaneous_information.pdf

Author Contributions

M.F.S. and S.B. equally contributed to the paper. M.F.S. and W.R. designed the study. M.B. and A.S. synthesized the samples and performed scattering experiments. M.F.S. performed the AFM measurements. S.B. developed the Force Volume data analysis. All authors took part in the discussion of the results and the completion of the manuscript.

Content Overview

The Supporting Information contains

Experimental Section, Bulk Solution Properties, Conventional Nanogels Imaged by Peak Force Tapping Mode, Corrected Height Images, Contact Stiffness vs. Indentation Depth, Contact Stiffness Map in Collapsed State, and Sample Code.

Additional supporting research data for this article may be accessed at no charge at

`https://hdl.handle.net/21.11102/d07925db-088e-11eb-afb2-e41f1366df48`.

Experimental Section

Materials

Poly(*N*-isopropylacrylamide) (PNIPAM) nanogels with 5 mol% cross-linker (*N*,*N*'-methylenebisacrylamide, BIS) content, referred to as conventional, and ultra-low cross-linked (ULC, 0 mol% BIS) nanogels were synthesized by Brugnoni resp. Scotti and Virtanen (for details of the synthesis protocol refer to Schulte et al.[1]). Glass substrates were modified with poly(allylamine hydrochloride) (PAH, Sigma Aldrich). If not stated differently, filtered (0.2 μm RC) double-distilled water was used as solvent.

Dynamic Light Scattering (DLS), Static Light Scattering (SLS), and Small-Angle Neutron Scattering (SANS)

The nanogels were analyzed in diluted bulk solution. For details regarding the DLS, SLS, and SANS measurements see Schulte et al.[1] The hydrodynamic radius as a function of temperature was extracted from DLS measurements. Scattering curves obtained from SLS and SANS measurements were fitted with the fuzzy-sphere form factor model [2] to extract the relative radial polymer volume fraction profiles. The data are provided in the Supporting Information (Figure S2).

Sample Deposition

The conventional and ULC nanogels were deposited onto PAH-coated glass substrates by *in situ* adsorption as published previously.[1] Briefly, glass coverslips with a size of $2.2 \times 2.2\,\mathrm{cm}^2$ (Menzel-Gläser, #4) were cleaned by ultrasonication in isopropanol for 15 min. The glass surface was activated by oxygen plasma treatment (PVA TePla plasma system 100) with 1.4 mbar oxygen pressure at 200 W of microwave power for 20 min. Four spin-coating steps were performed on a Convac 1001S spin-coater at 2500 rpm for 30 s each. The activated glass substrate was first coated with 120 μL of an aqueous PAH-solution ($c_{\mathrm{monomer}} = 0.1\,\mathrm{M}$). Three spin-coating steps with 500 μL of water were performed to remove excess polymer. Immediately, the PAH-coated glass coverslip was placed in a customized liquid cell of the AFM. 500 μL of nanogel solution (ice-cooled) were dropped onto the substrate and incubated for 30 min at a temperature of $T = 27\,^{\circ}\mathrm{C}$. The mass concentration of the conventional nanogels was 0.025 wt% and of the ULC nanogel solution 0.005 wt% (the freeze-dried nanogels were redispered in water). Excess of nanogel was removed by extensive rinsing with water. The substrates were kept under water without letting them dry for AFM measurements at the solid/liquid interface.

AFM Measurements

AFM measurements were performed on a Dimension Icon AFM with a closed loop (Veeco Instruments Inc., software Nanoscope 9.4 (Bruker Corporation)). Investigations at the solid/liquid interface were conducted in a customized liquid cell on a heating stage (Dimension Icon Electrochemistry Chuck, Bruker Corporation) with temperature control (Model 335 Cryogenic Temperature Controller, Lake Shore Cryotronics).

A 55 μm thick polyimide-foil was placed beneath the glass substrate on the detector side before *in situ* deposition of the nanogels. The nanogels were analyzed at $T = 27$, and $35\,^{\circ}\mathrm{C}$. The temperature was equilibrated for 60 min. For the ULC nanogels, a temperature cycle was performed starting at $T = 35\,^{\circ}\mathrm{C}$, lowering the temperature in $2\,^{\circ}\mathrm{C}$-steps until $T = 27\,^{\circ}\mathrm{C}$

was reached, and heating again to $T = 35\,^{\circ}\mathrm{C}$ with an equilibration time of 20 min for the short temperature intervals.

The measurements were performed in the Peak Force QNM and Force Volume mode with modified MSNL (Bruker Corporation) tips. The AFM tips were activated by oxygen plasma treatment (PVA TePla plasma system 100) with 1.4 mbar oxygen pressure at 200 W microwave power for 5 min. Immediately, the tip was used for AFM measurements. The D and E probes with a nominal resonance frequency of 15 and 38 kHz in air and a nominal spring constant of 0.03 and 0.1 N/m of the cantilever, respectively, were used (tip radius: 2 nm, semi angle of the tip: 23°, assumed sample Poisson's ratio: 0.3).

The tips were calibrated before use. Force-spectroscopy measurements on the bare solid substrate were conducted. The cantilever deflection sensitivity was determined from the slope of the deflection-distance-curve after the contact point. The tip was withdrawn from the surface by 1000 μm and the thermal noise was measured by the thermal tune of the Nanoscope 9.4 software, giving rise to the cantilever spring constant. The conventional nanogels were characterized with MSNL-E probes with a sensitivity $Sens = 68.60\,\mathrm{nm/V}$ and a spring constant $k = 0.11\,\mathrm{N/m}$ and the ULC nanogels with MSNL-D probes ($Sens = 106.7\,\mathrm{nm/V}$, $k = 0.04\,\mathrm{N/m}$).

Operating the AFM in the Peak Force QNM mode, the integrated ScanAsyst was used to control the feedback in terms of z-limit. The measurements in the collapsed state ($T = 35\,^{\circ}\mathrm{C}$) are the identical as reported previously.[1] Table S1 summarizes the Peak Force QNM mode scan parameters, which were set manually (amplitude A, frequency f, setpoint SP, and gain), for all swelling states.

Force Volume mode measurements were performed for stiffness tomography in analogy to previous studies.[3–6] In contrast to the Peak Force QNM mode, the velocity of the probe during the individual force-distance curve measurement is constant, here. Force Volume mode measurements were conducted with a scan size of $2.0 \times 2.0\,\mu\mathrm{m}^2$ and 192×192 data points in a sample region with at least three intact nanogels. The measurements were

Table S1: Peak Force scan parameter used for the measurements of the adsorbed nanogels at the solid/liquid interface at different temperatures. The conventional and ULC nanogels were deposited via *in situ* adsorption. The Peak Force scan parameter are specified in terms of Peak Force amplitude A, frequency f, setpoint SP, and gain.

sample type		**Peak Force scan parameter**			
		A [nm]	f [kHz]	SP[nN]	Gain
conventional	T = 27 °C	200	1.0	0.5	15.0
	T = 35 °C	200	1.0	1.0	10.0
ULC	T = 27 °C	200	0.125	0.3	0.9
	T = 29 °C	200	0.25	0.3	2.0
	T = 31 °C	200	0.25	0.5	3.0
	T = 33 °C	200	0.25	0.5	3.0
	T = 35 °C	200	0.25	0.5	3.0

performed with a force threshold of $F = 0.3\,\mathrm{nN}$ for the ULC at $T = 27\,^{\circ}\mathrm{C}$ resp. 1.0 nN at $T = 35\,^{\circ}\mathrm{C}$, and 5.0 nN for the conventional nanogels in both swelling states. The ramp size was 500 nm, the ramp rate 10 Hz, and the number of samples 3072. Measurement data were extracted by the Nanoscope Analysis 1.9 Software (Bruker Corporation) for further analysis.

Force Volume Data Analysis

Force-spectroscopic measurements allow the quantification of mechanical properties of the sample. While single force-distance curves can be evaluated by hand, the analysis of a huge amount of data sets as obtained by force mapping in a Force Volume mode measurement (here, $192 \times 192 = 36864$ curves per scan) requires a robust batch evaluation routine to obtain information in a reasonable time. Available software, however, fails in the analysis of low signal-to-noise ratio data - the case of the ULC nanogels in the swollen state. Therefore, a custom-made MATLAB routine (MathWorks, 2020a) was developed.

In a first step, all curves are first-order baseline corrected. An input parameter allows the user to specify the relative amount of data points used for leveling, which should represent the non-contact region of the sample and tip ($F = 0$). Typically, the first 50% of the curves were used for the correction.

Secondly, the MATLAB routine distinguishes force-distance curves sensing the interaction with the bare substrate and the sample. In this manner, the last points of the individual curves are fitted to a line with the cantilever stiffness as the slope. The intersection of this line and the baseline ($F = 0$) is determined. If a significant number of data points between the beginning and the intersection displays certain force values above a user-defined threshold, the curve is considered to contain relevant data, i.e., the probe is interacting with the sample. Otherwise, the curve is assigned to the interaction of the probe and the bare substrate and is not further analyzed.

Next, the contact point is determined for each curve by the routine. The contact point corresponds to the vertical position of the AFM probe at which sample and tip start to interact so that the force deviates from zero. Small changes of the force value are detected based on the CUSUM (**cu**mulative **sum**) method. The method is well-established for sequential analysis and typically used to keep time-dependent processes on target. Briefly, the variation from the target is detected by the standard deviations of the means. CUSUM is implemented by the *cusum* function in MATLAB. With a target of zero force, this function allows the determination of the contact point for noisy data. The contact point is determined for each curve which is then shifted to a distance value of zero, accordingly. In this manner, force vs. indentation depth curves are obtained. Individual curves at desired positions can be extracted as plotted in Figure 2 for five positions across the ULC nanogels and in Figure 4 for the nanogels' center.

AFM imaging relies on the sensing of forces. Within the Force Volume measurements a force threshold is set and kept constant by the feedback mechanism. A topographic map is obtained based on the difference of the probe's z-position to reach this threshold. While a hard surface is connected to a steep increase in force, soft samples like nanogels are strongly indented by low forces (e.g., the application of 100 pN results in an indentation of 150 nm for the ULC nanogels in the swollen state, see Figure 4A, gray open circles). Even though the force threshold for mapping is kept to a minimum, strong indentation into soft samples

cannot be prevented. As a result, the imaged topography is incorrect. To reveal the true surface (with the limit of a sensible force) the height images have to be corrected by the indentation depth resulting from the application of the force. The custom-written routine calculates this indentation depths by the difference in the distance values between $F = 0$, i.e., the determined contact point, and the distance at which the force threshold is reached. The previous height image is corrected by adding the individual indentation depth value in every pixel. Figure S4 shows the corrected height images as received for the ULC and conventional nanogel in the swollen and collapsed state.

To gather information beyond the surface of the sample, the data are further evaluated by the routine. Firstly, the force values of each force-indentation depth curve are averaged for a user-defined range of data points (typically 1-3% of total data points). Here, all curves were evaluated with an averaging value of 3% corresponding to ca. 10 nm in distance. In a next step, the first derivative of the averaged force-indentation depth curves is determined. The first derivative corresponds to a contact stiffness. Since the sharp AFM probe is penetrating the porous nanogel networks the local contact stiffness is a measure of the network density.[7] The corresponding contact stiffness-indentation depth curves can be plotted for selected positions. Figure S5 shows the contact stiffness profiles of the ULC and conventional nanogels in swollen and collapsed state as determined at the nanogel center.

The force or contact stiffness as a function of the indentation depth cannot only be plotted in one point of the scanned area. Finally, the routine allows the three-dimensional visualization of the Force Volume data. Figure S1 shows the three-dimensional force map as obtained for the ULC and conventional nanogels in swollen and collapsed state. The corresponding contact stiffness maps are given in Figures 5 and S6.

For the three-dimensional maps, all force and contact stiffness values for $d < 0$ nm, i.e., in the non-contact region, are zeroed. The MATLAB function *isosurface* is used to extract a surface of identical value from the volume data. This value is set to zero force resp. contact stiffness and the extracted surface is plotted in light blue. To image the internal structure

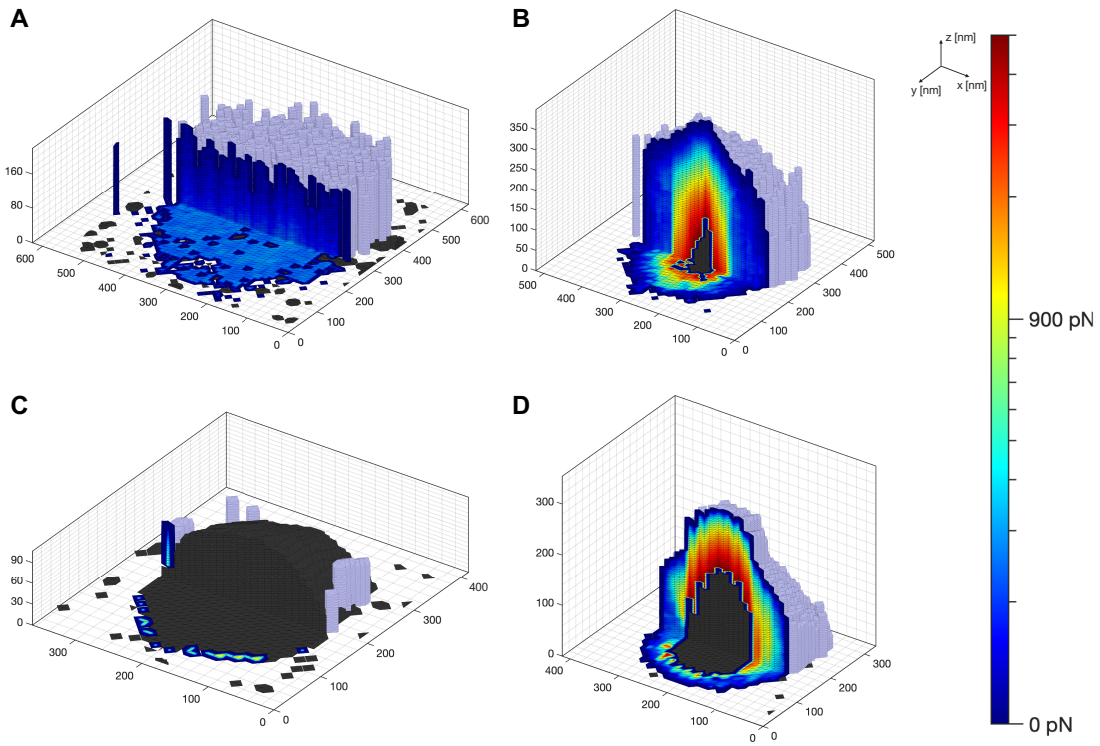

Figure S1: Cut-offs of the force maps of individual ULC (A and C) and conventional (B and D) nanogels at the solid/liquid interface at $T = 27\,^{\circ}\mathrm{C}$ (A and B) and $35\,^{\circ}\mathrm{C}$ (C and D). The x, y, and z-axes describe the topographic information (light blue surface extracted for $F = 0\,\mathrm{pN}$), while the color code within the cut-off planes signifies the local contact stiffness value. The dark gray color reflects the area which cannot be accessed by the AFM tip.

cut-offs through the nanogels are formed and the resulting caps (MATLAB function *isocaps*) are signified by different colors according to its force/contact stiffness value. Since the samples (except the ULC nanogels in swollen state) are not entirely indented, the region inaccessible by the probe is represented in dark gray. This dark gray region corresponds to the conventionally imaged topography (without the correction by the indentation depth).

Examplarly, a Macbook Pro mid 2015 with a 2.2 GHz Quad-Core Intel Core i7 processor (Apple Inc.) evaluates 36864 force-distance curves in less than 10 min.

Bulk Solution Properties

The structure of the conventional and ULC nanogels was determined in dilute aqueous solution in the swollen and collapsed states, i.e., at temperatures below and above the volume phase transition temperature (VPTT), by means of dynamic (DLS) and static light scattering (SLS) as well as by small-angle neutron scattering (SANS). Figure S2A shows the hydrodynamic radii as a function of the temperature determined from DLS. The scattering curves from SLS and SANS measurements are given in Figures S2B and C and were fitted with the fuzzy-sphere model.[2] The relative polymer volume fraction as a function of the radial position within the nanogel were determined by the fits and are shown in Figures S2D and E.

The ULC nanogels exhibit box-like polymer density profiles with a hydrodynamic radius of $R_{h,40\,^\circ C} = 118 \pm 2\,\mathrm{nm}$ in the collapsed state (Figure S2A, grey open circles). Upon temperature decrease across the volume phase transition temperature (VPTT = 32 °C), the nanogels swell by a factor of 3.3 ± 0.2 ($R_{h,20\,^\circ C} = 385 \pm 22\,\mathrm{nm}$). The swelling is accompanied by a change of the internal polymer density profile (Figure S2E); (i) the swollen nanogels resemble fuzzy spheres with a fuzziness of 15%, and (ii) the polymer density reduces by a factor of ca. 30 in the center of the nanogel. In contrast to conventional nanogels, the different and ultra-soft character of ULC nanogels can be concluded by two facts: firstly, the internal structure of conventional nanogels in the swollen state is more heterogeneous with a fuzzy periphery with decaying polymer density of about 70% of the total radius (Figure S2D, black line). The heterogeneous core-corona structure is a result of the faster polymerization of the cross-linking molecules compared to the main monomer NIPAM.[2] Secondly, conventional nanogels exhibit a much lower degree of swelling (ratio between $R_{h,20\,^\circ C}$ and $R_{h,40\,^\circ C}$) of only 1.8 ± 0.1. However, both nanogels have a similar hydrodynamic radius as well as internal structure in the collapsed state.

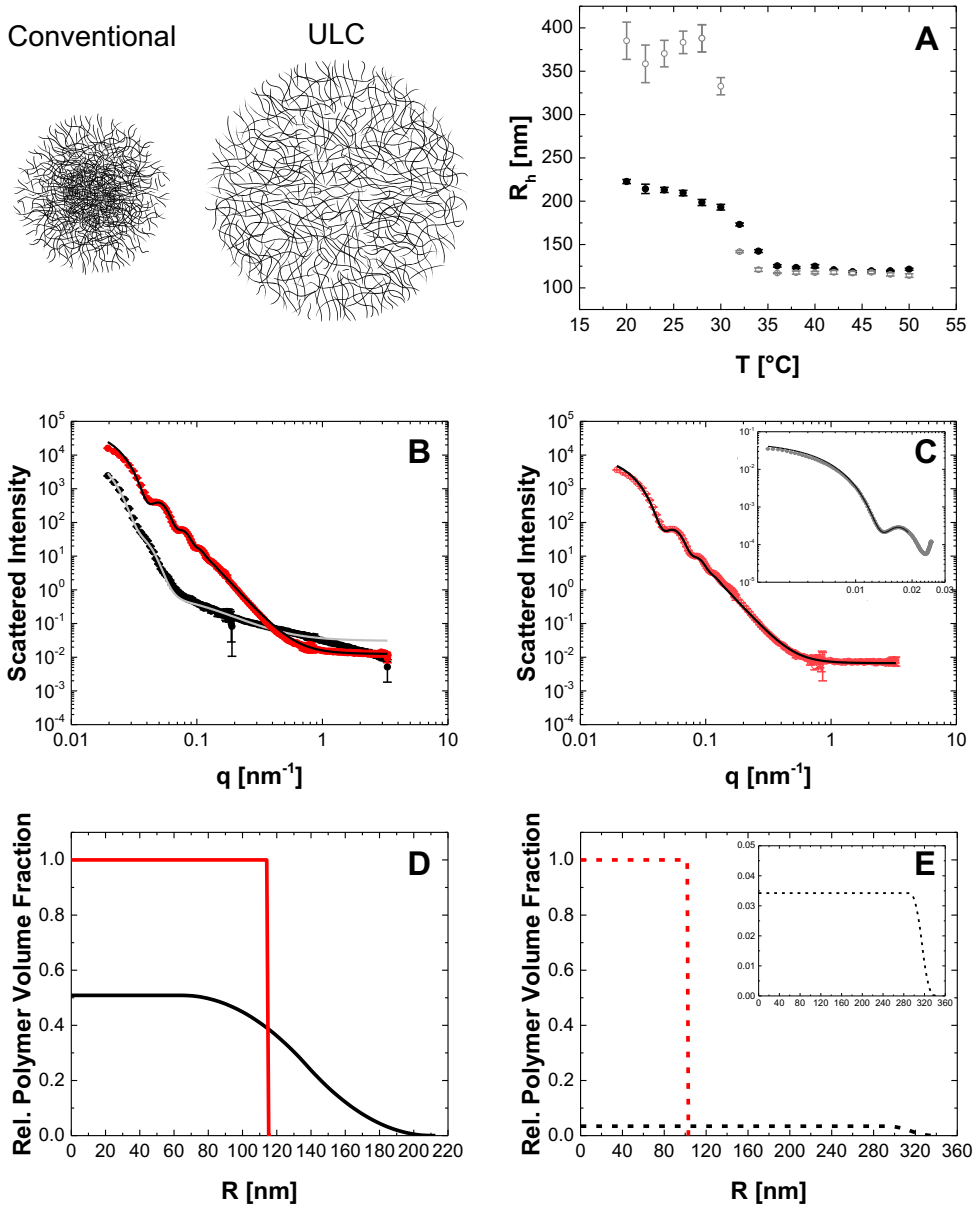

Figure S2: Schematic illustration of the conventional and ULC nanogels in bulk solution in the swollen state. A: Hydrodynamic radii R_h as a function of the temperature T of the conventional (black filled circles) and ULC (gray open circles) nanogels in H_2O studied by DLS. B and C: Form factors probed by SANS of the conventional (B, filled circles) and ULC (C, open circles) nanogels at $T = 20\,^{\circ}\mathrm{C}$ (black/gray) and $T = 40\,^{\circ}\mathrm{C}$ (red/light red). The data were fitted with the fuzzy-sphere model [2] and are represented by the solid lines (gray/ black). Inset in C: Form factor of ULC nanogels at $T = 20\,^{\circ}\mathrm{C}$ was probed by SLS as they are too large to be analyzed by SANS. D and E: Relative polymer volume fraction versus radial position R, as obtained from the SLS/SANS form factor fits for conventional (D, solid lines) and ULC nanogels (E, dashed lines) at $T = 20\,^{\circ}\mathrm{C}$ (black) and $T = 40\,^{\circ}\mathrm{C}$ (red). Inset in E: Zoom of the relative polymer volume fraction versus R for the ULC nanogels below the VPTT ($T = 20\,^{\circ}\mathrm{C}$).

Conventional Nanogels Imaged by Peak Force Tapping Mode

Conventional nanogels were adsorbed *in situ* at $T = 27\,^{\circ}\mathrm{C}$ onto a PAH-coated glass substrate and investigated at temperatures above and below the VPTT at the solid/water interface. Topographic images were taken in the Peak Force tapping mode applying a minimum force to obtain a stable image ($SP = 1.0/0.5\,\mathrm{nN}$, Figure S3).

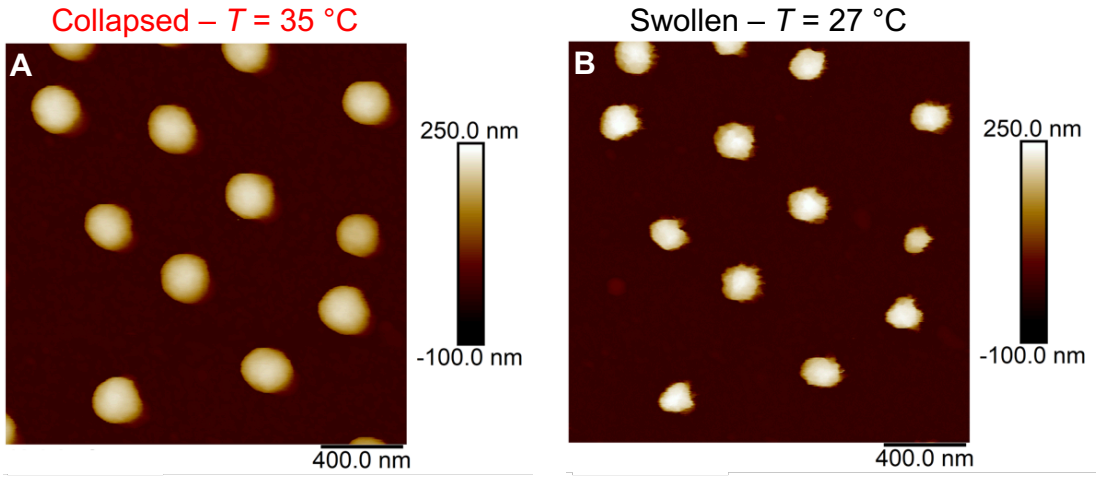

Figure S3: AFM height images of the conventional nanogels *in situ* adsorbed on a PAH-coated glass substrate in the hydrated state. The measurements at temperatures above (A, $T = 35\,^{\circ}\mathrm{C}$) and below (B, $T = 27\,^{\circ}\mathrm{C}$) the VPTT were obtained at the same position by Peak Force tapping mode measurements with an applied force of $SP = 1.0$ resp. $0.5\,\mathrm{nN}$.

Figure S3A shows the height image of the conventional nanogels in the collapsed state at $T = 35\,^{\circ}\mathrm{C}$. As reported previously,[1,8] the nanogels exhibit half-ellipsoidal shapes. In the swollen state ($T = 27\,^{\circ}\mathrm{C}$, Figure S3B), a smaller force ($SP = 0.5\,\mathrm{nN}$) was applied during imaging to reduce the impact on the imaged morphology. However, the nanogels exhibit a more rough surface structure and appear to be smaller in lateral dimensions in comparison to the collapsed state. This highlights the strong influence of the imaged morphology by

the application of a force [7,9] and the necessity of the correction of the height information by the indentation depth - being of significant relevance in the swollen state. Nonetheless, the conventional nanogels are still locatable by imaging in the Peak Force tapping mode which is in strong contrast to the ultra-soft ULC nanogels (Figure 1E).

Corrected Height Images

A topographic image within force mapping modes of an AFM is created by the difference in z-position needed to reach a threshold force value, i.e., the imaging is connected to the sensing of forces. A hard surface is easily recognized due to the strong increase in force for small vertical movements of the fixed-end of the cantilever. In contrast, the application of low forces on soft samples results in a significant indentation into the material. Therefore, the imaged morphology strongly differs from the real surface of the sample and a correction of the image is required. The force-distance curves recorded in every pixel of Force Volume mode images are used to quantify the height information missed due to the application of the threshold force (see exemplary Figure 2I-V). Figure S4 shows the corrected height images of the ULC and conventional nanogels in the swollen and collapsed state.

For both nanogel types in the collapsed state (Figures S4A and C), the corrected height image is similar to the images directly obtained by the Peak Force tapping mode (see Figures 1A and S3A for the ULC and conventional nanogels, resp.). It shows that the indentation into the collapsed nanogel network is strongly limited and the application of a force is leading to small indentations only, i.e., the correction is only minor.

In the swollen state, however, the effect of the applied force is significant (Figures S4B and D). While the swollen ULC nanogels are not directly mappable via Peak Force tapping mode measurements (Figure 1E), also for the conventional nanogels a strong difference between the directly obtained and the corrected height image is present (Figures S3B and S4D, resp.). Even if the applied force is kept to a minimum, strong indentation into the nanogels in swollen state cannot be prevented. The nanogels are an open and porous system in which the sharp AFM tip is penetrating. This significant difference between uncorrected and corrected height images highlights the necessity of the correction of the topographic information for soft samples.

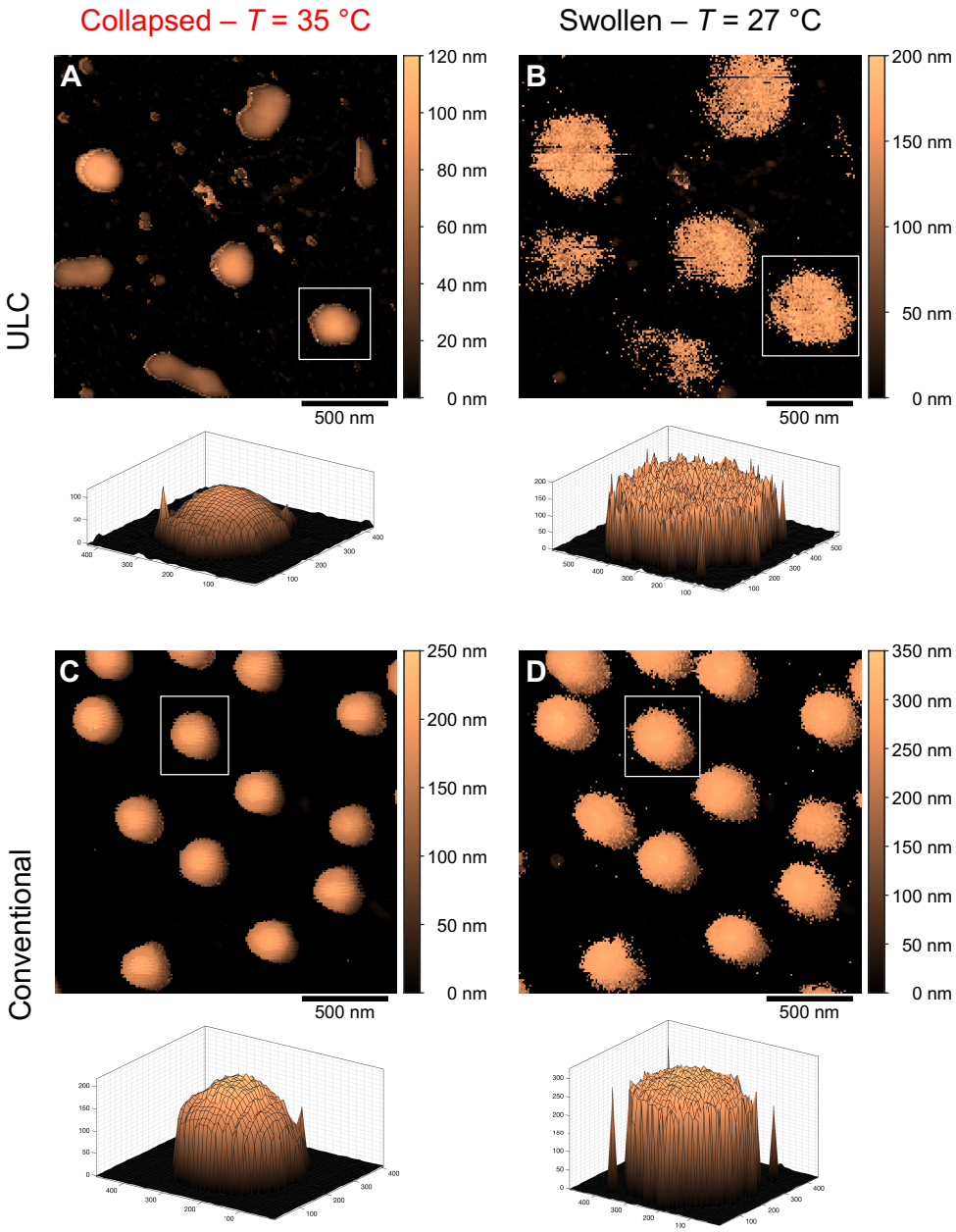

Figure S4: Corrected height image of the ULC (A and B) and the conventional nanogels (C and D) *in situ* adsorbed onto a PAH-coated glass substrate in water. The measurements at $T = 35\,°C$ (A and C), and at $T = 27\,°C$ (B and D) were obtained at the same position. The height information is corrected by the indentation depth in every pixel due to the application of a force of $F = 1.0\,nN$ (A), $0.3\,nN$ (B), and $5.0\,nN$ (C and D) for imaging via the Force Volume mode. Note the difference in the z-scale for the individual images. Below each image, a three-dimensional height map (x, y, and z in nanometer) of a single nanogel is given (the white rectangle marks the corresponding section in the image above).

Contact Stiffness vs. Indentation Depth

Force-spectroscopic measurements allow the quantification of mechanical properties of a sample. For nanogels in the swollen state, a sharp AFM tip instead of compressing the sample is penetrating the meshes of the nanogel network.[7] Therefore, during the vertical movement of the probe a local penetration resistance is monitored. The first derivative of the force is a contact stiffness - a measure for the polymer segment density in vertical direction. This polymer density distribution orthogonal to the interface is compared to the polymer density profiles of the nanogels in diluted bulk solution as determined by SLS and SANS - interfacial and bulk solution properties are correlated. Figure S5 shows the contact stiffness as a function of the indentation depth (red/black curve, first derivative of the force-distance curves of Figure 4) as well as the relative polymer volume fraction as a function of the radial position (green curve) for the ULC and conventional nanogels in the collapsed and swollen state.

The ULC nanogels in the collapsed state are only indented by a few nanometer ($\Delta d <$ 5 nm) due to the application of a 1.0 nN force (Figure S5A, red dashed curve). Nonetheless, the limited probed periphery reveals a steep increase of the contact stiffness being in agreement with the box-like density profile in bulk solution (Figure S5A, green dashed curve).

Similar to the ULC nanogels, the conventional nanogels in the collapsed state possess a steep increase of the contact stiffness, too, reaching a value of ca. 500 pN/nm at an indentation depth of 70 nm (Figure S5B, red curve). Both nanogel types have the strongly increasing contact stiffness with an increasing indentation for $T >$ VPTT in common - correlating with their identical size and internal structure in bulk solution.

In contrast, the internal density profiles in the swollen state ($T <$ VPTT) disclose a significant difference between the two nanogel species (Figures S5C and D). With a minimum force of only 100 pN, the entire ULC nanogel gets penetrated by the tip. The low signal-to-noise ratio of the force-distance curve results in an amplification of the noise for the contact stiffness-indentation depth curves due to the differentiation (inset in Figure S5C,

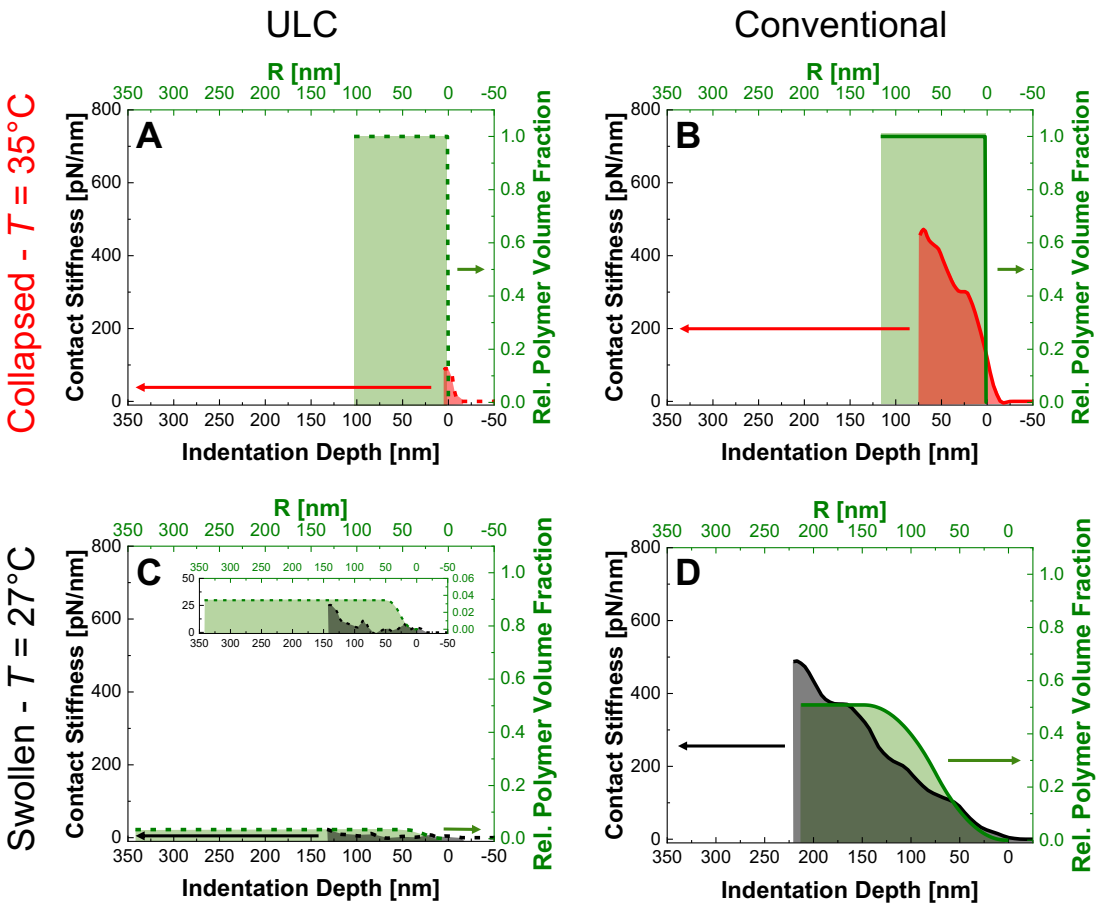

Figure S5: Contact stiffness (first derivative of the force-distance curves, Figure 4) vs. indentation depth plotted on the left and bottom axis (black), and polymer density from SLS/SANS measurements (green curves, A and B: $T = 40\,^{\circ}\mathrm{C}$, C and D: $T = 20\,^{\circ}\mathrm{C}$) vs. radial position within the nanogel plotted on the right and upper axis (green). Zero radial position signifies the nanogels' periphery. The contact stiffness curves are shown for the ULC (A and C, solid lines) and conventional nanogels (B and D, dashed lines) at $T = 35\,^{\circ}\mathrm{C}$ (A and B, red) and $T = 27\,^{\circ}\mathrm{C}$ (C and D, black). Inset in C: Zoom-in graph to visualize the scale of interest for the ULC nanogels in the swollen state.

black dashed curve). Within the whole penetration region ($\Delta d \approx 150\,\mathrm{nm}$), the contact stiffness varies between 0 and $25\,\mathrm{pN/nm}$, i.e., it is very small and nearly constant with respect to the relevant scale for all other samples. The low and constant contact stiffness value is in agreement with the homogeneous and very low polymer density in bulk solution.

The differences between the ULC and conventional nanogels in the swollen state is manifested by two facts: Firstly, not the whole conventional nanogel is penetrated by the sharp

AFM tip, as indicated by the absence of the steep increase in force attributed to the contact between the tip and the solid substrate (Figure 4B). Secondly, for the entire probed region ($\Delta d = 0 - 230\,\mathrm{nm}$) the contact stiffness is monotonically raising from $0\,\mathrm{pN/nm}$ at the nanogels' periphery up to ca. $500\,\mathrm{pN/nm}$ at the highest penetration (Figure S5D). Also for the structure in bulk solution, an increase of the polymer volume fraction towards the nanogel center is observed (fuzzy-sphere architecture [2]), i.e., the typical heterogeneous structure of the conventional nanogels persists at the interface.

Contact Stiffness Map in Collapsed State

The internal structural information cannot only be extracted in one point if Force Volume mode measurements are performed. Within these measurements, a 192×192 array of force-distance curves was measured across a $2.0 \times 2.0\,\mu m^2$ scan area. Instead of the single curve, the full information can be plotted in a map. Figure S6 shows the cut-offs of the extracted contact stiffness maps of the ULC (A) and conventional nanogels (B) in the collapsed state.

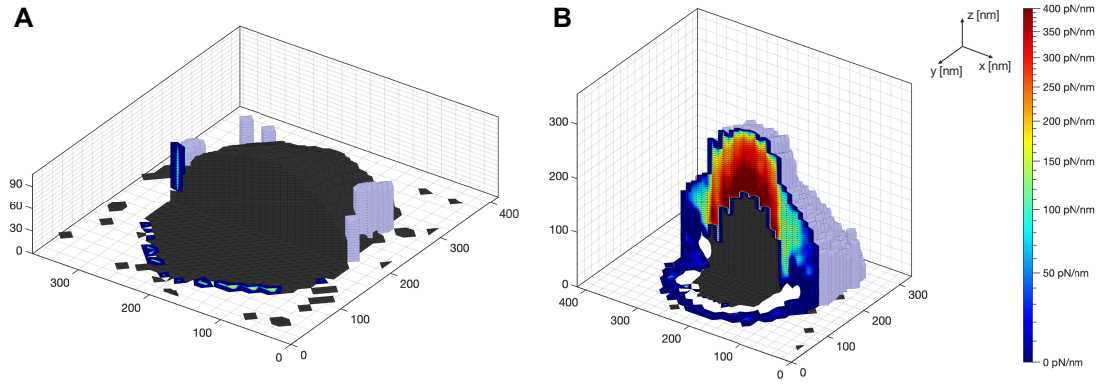

Figure S6: Cut-offs of the contact stiffness maps of individual ULC (A) and conventional (B) nanogels at the solid/liquid interface at $T = 35\,°C$. The x, y, and z-axes describe the topographic information (light blue surface extracted for contact stiffness equals $0\,pN/nm$), while the color code within the cut-off planes signifies the local contact stiffness value. The dark gray color reflects the area which cannot be accessed by the AFM tip and white the regions of negative contact stiffness.

On one hand, the topographic information is signified by the x, y, and z-axes. The light blue surface represents the surface of the individual nanogels. It is determined from the individual z-positions in space where the contact stiffness equals zero. On the other hand, the internal contact stiffness values within the cut-off planes are captured by a color code. While regions of low contact stiffness are marked in blue, regions of higher contact stiffness are colored in red, and a negative stiffness value is represented by a white coloration. Especially in the collapsed state, not the entire samples can be probed by the AFM tip. The inaccessible area is colored in dark gray and corresponds to the directly imaged topography (without the correction by the indentation depth). For details regarding the processing of the Force Volume data refer to Section *"Force Volume data analysis"* of the Experimental

Section.

As already observed by the force-distance curve in the nanogel center (Figure 4A, light red open circles), the probable area of the ULC nanogels in the collapsed state is nearly zero (Figure S6A). The entire cut-off planes are colored in dark gray, i.e., no internal structural information is received.

For the conventional nanogels (Figure S6B), a part of the collapsed network can be probed. While a vertical change of the contact stiffness is absent, a significant gradient along the lateral direction is observed. The stiffness is lowest (ca. 20 pN/nm) at the periphery and increases toward the nanogel center up to ca. 400 pN/nm. It is expected that the nanogel networks densifies in the collapsed state. This densification explains the absence of a vertical stiffness gradient, correlating with the box-like density profile in bulk solution.

Sample Code

The conventional nanogels were synthesized by Monia Brugnoni and have the sample code: MB-pNIPAM-5mol%BIS-225nm/SFB985_A3_MB_M000186. The ultra-low cross-linked (ULC, 0 mol% BIS) nanogels were synthesized by Andrea Scotti and possess the sample code: SCOT1-ULC/SFB985_A3_SCO_M000508.

References

(1) Schulte, M. F.; Scotti, A.; Brugnoni, M.; Bochenek, S.; Mourran, A.; Richtering, W. Tuning the Structure and Properties of Ultra-Low Cross-Linked Temperature-Sensitive Microgels at Interfaces via the Adsorption Pathway. *Langmuir* **2019**, *35*, 14769–14781.

(2) Stieger, M.; Richtering, W.; Pedersen, J. S.; Lindner, P. Small-angle neutron scattering study of structural changes in temperature sensitive microgel colloids. *J Chem Phys* **2004**, *120*, 6197–206.

(3) Roduit, C.; Sekatski, S.; Dietler, G.; Catsicas, S.; Lafont, F.; Kasas, S. Stiffness tomography by atomic force microscopy. *Biophys J* **2009**, *97*, 674–677.

(4) Roduit, C.; Saha, B.; Alonso-Sarduy, L.; Volterra, A.; Dietler, G.; Kasas, S. OpenFovea: open-source AFM data processing software. *Nat Methods* **2012**, *9*, 774–5.

(5) Longo, G.; Rio, L. M.; Roduit, C.; Trampuz, A.; Bizzini, A.; Dietler, G.; Kasas, S. Force volume and stiffness tomography investigation on the dynamics of stiff material under bacterial membranes. *J Mol Recognit* **2012**, *25*, 278–284.

(6) Galluzzi, M.; Tang, G.; Biswas, C. S.; Zhao, J.; Chen, S.; Stadler, F. J. Atomic force microscopy methodology and AFMech Suite software for nanomechanics on heterogeneous soft materials. *Nat Commun* **2018**, *9*, 3584.

(7) Schulte, M. F.; Scotti, A.; Gelissen, A. P. H.; Richtering, W.; Mourran, A. Probing the Internal Heterogeneity of Responsive Microgels Adsorbed to an Interface by a Sharp SFM Tip: Comparing Core-Shell and Hollow Microgels. *Langmuir* **2018**, *34*, 4150–4158.

(8) Schmidt, S.; Zeiser, M.; Hellweg, T.; Duschl, C.; Fery, A.; Möhwald, H. Adhesion and Mechanical Properties of PNIPAM Microgel Films and Their Potential Use as Switchable Cell Culture Substrates. *Adv Funct Mater* **2010**, *20*, 3235–3243.

(9) Aufderhorst-Roberts, A.; Baker, D.; Foster, R. J.; Cayre, O.; Mattsson, J.; Connell, S. D. Nanoscale mechanics of microgel particles. *Nanoscale* **2018**, *10*, 16050–16061.